32ND INTERNATIONAL COSMIC RAY CONFERENCE, BEIJING 2011

AERA: the Auger Engineering Radio Array

JOHN L. KELLEY[1] FOR THE PIERRE AUGER COLLABORATION[2]
[1]*IMAPP / Dept. of Astrophysics, Radboud University Nijmegen, 6500GL Nijmegen, Netherlands*
[2]*Observatorio Pierre Auger, Av. San Martín Norte 304, 5613 Malargüe, Argentina*
(Full author list: http://www.auger.org/archive/authors_2011_05.html)
auger_spokespersons@fnal.gov

Abstract: The first part of the Auger Engineering Radio Array, presently consisting of 21 radio-detection stations, has been installed in the surface detector array of the Pierre Auger Observatory and in close proximity to the fluorescence detectors Coihueco and HEAT. In the coming years, the number of detection stations will grow to 160 units covering an area of almost 20 square kilometers. AERA is sensitive to radio emission from air showers with an energy threshold of 10^{17} eV and is being used to study in detail the mechanisms responsible for radio emission in the VHF band. The design of AERA is based on results obtained from prototype setups, with which we investigated triggering methods and different hardware concepts. We present the first data from AERA, including AERA's first hybrid radio / particle detector events.

Keywords: radio, air shower, hybrid, AERA, Pierre Auger Observatory

1 Introduction

The radio detection of cosmic ray air showers offers a scalable, high-duty-cycle approach for the next generation of air shower arrays. Broadband radio pulses from air showers are coherent in the VHF band (10-100 MHz) and thus have a signal power which scales with the square of the cosmic ray primary energy. The pulse characteristics can be used to probe the electromagnetic shower development and primary particle composition [1, 2]. Recent experiments such as LOPES [3] and CODALEMA [4] have employed antennas triggered by particle detectors to demonstrate the method and verify the dominant emission mechanism — the acceleration of shower particles in the Earth's magnetic field. At the same time, significant progress has been made in the theoretical understanding of the radio signals [5], with current work focused on the more subtle sub-dominant emission mechanisms.

A technical challenge has been to develop a large-scale, autonomous antenna array which triggers directly on the radio pulses (a "self-triggered" array). At the same time, more measurements are needed to fully understand the radio signal polarization and lateral distribution, and thus to continue to refine theoretical models. The deployment of the Auger Engineering Radio Array (AERA) has started in 2010 at the Pierre Auger Observatory in Argentina, in order to address these technical and scientific issues. Stable physics data-taking has begun in March 2011, and the first hybrid radio/particle detector events have been recorded in April 2011.

2 AERA

AERA is a radio extension of the Pierre Auger Observatory. The observatory is a 3000-km^2 hybrid cosmic ray air shower detector in Argentina, with an array of 1660 water-Cherenkov detectors and 27 fluorescence telescopes at four locations on the periphery. The area near the Coihueco fluorescence detector contains a number of low-energy enhancements, including the AMIGA infill array [6] and the HEAT fluorescence telescopes [7]. AERA is co-located with the infill water-Cherenkov detectors and within the field of view of HEAT, allowing for the calibration of the radio signal using "super-hybrid" air shower measurements.

Stage 1 of AERA consists of 21 radio-detection stations (RDS) arranged on a triangular grid with 150 m spacing. Stages 2 and 3, with larger detector spacings of 250 m and 375 m, will increase the total area covered to nearly 20 km^2 (see Fig. 1).

AERA has an energy threshold of approximately 10^{17} eV, with its fundamental noise limit set by the radio emission from the Galactic plane. The scientific goals of the experiment are as follows:

- calibration of the radio emission from the air showers, including sub-dominant emission mechanisms, by using super-hybrid air shower measurements;
- demonstration of the physics capabilities of the radio technique, *e.g.* energy, angular, and primary mass resolution; and

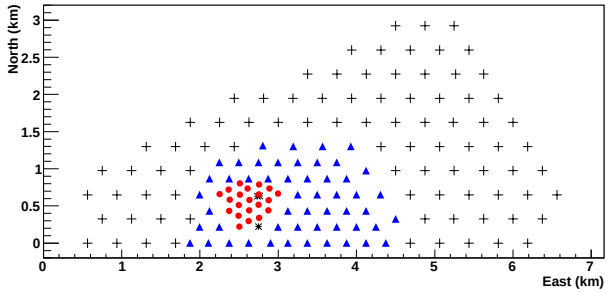

Figure 1: Layout of AERA radio-detection stations. The Stage 1 core stations (solid circles) were deployed in 2010. Planned expansions (solid triangles, crosses) will increase the instrumented area to nearly 20 km^2.

- measurement of the cosmic ray composition in the ankle region, from 0.3 to 5 EeV, with the goal of elucidating the transition from Galactic to extra-Galactic cosmic rays.

2.1 Radio-Detection Station

The AERA Stage 1 radio-detection stations (RDS) consist of an antenna, associated analog and digital readout electronics, an autonomous power system, and a communications link to a central data acquisition system. The RDS design has been informed by the results of several prototype setups at the Auger site, with progress in antenna design, noise filtering, and self-triggering by radio detection stations at the Balloon Launching Station [8, 9] and the Central Laser Facility [10, 11].

The RDS antenna is a dual-polarization log-periodic dipole antenna, oriented to point north-south and east-west. The antenna is sensitive between 27 and 84 MHz, chosen as the relatively radio-quiet region between the shortwave and FM bands. The north-south and east-west antenna signals are separately amplified with two low-noise amplifiers (LNAs), each with a gain of 20 dB. The LNAs incorporate a bandpass filter (23-79 MHz) to eliminate any issues with intermodulation from the FM band.

The amplified antenna signals are routed into a custom aluminum housing containing the bulk of the station electronics. The housing includes a radio-frequency-tight chamber to mitigate issues with self-generated noise. Inside the housing, the signals are further amplified and filtered with a custom bandpass filter (30-78 MHz). Both a low-gain (+10 dB) and high-gain (+19 dB) version of each polarization is generated, to increase the dynamic range of the station.

The four analog output channels of the filter-amplifier are then digitized with a custom 12-bit 200 MHz digitizer. The digitizer employs an FPGA with specially designed filtering and triggering logic using the time-domain radio signals. Several digital notch filters can be configured to remove remaining narrowband interference before triggering. The triggering logic employs multiple voltage thresholds in order to reject signals with afterpulsing. Once a trigger is recorded, up to 2048 voltage samples of each channel are stored for transfer to the central data acquisition system (DAQ), corresponding to 10.2 μs of data. Timestamping of the triggers is performed using an on-board GPS receiver.

The station is powered using a photovoltaic system with two storage batteries. For stage 1, communication to the central DAQ is via an optical fiber network. A high-speed, low-power wireless communications system is currently under development for the next stages.

2.2 Data Acquisition

The central data acquisition system (DAQ) is located in a central container, the Central Radio Station (CRS). The CRS is powered by its own photovoltaic array and is equipped with a weather station to monitor the local electric field (thunderstorm conditions amplify the air shower radio signal; see *e.g.* Ref. [12]).

All timestamps from single RDS triggers are sent to the central DAQ. A multi-station trigger is formed when neighboring stations trigger within a time window consistent with a signal moving at the speed of light across the array. Once a coincidence is formed, the full radio signals are read from the stations and stored to disk for analysis.

Trigger rates are highly dependent on the RDS thresholds and the local noise conditions, but on average, the RDS trigger rates are $\sim$ 100 Hz, while the multi-station trigger rate is $\sim$ 10 Hz. The vast majority of these triggers can be localized using the RDS data to sources on the horizon — that is, man-made radio-frequency interference (RFI). A number of techniques are incorporated into the DAQ to reject RFI sources at trigger level, based on direction and periodicity.

2.3 Beacon

A multi-frequency narrowband transmitter ("beacon") installed at the Coihueco fluorescence detector site transmits signals to AERA for timing calibration. Using the beacon frequencies as a phase reference, relative offsets in the individual RDS timestamps can be corrected, improving the timing resolution [13]. The transmitter signals are visible in the dynamic spectrum shown in Fig. 2.

3 Calibration, Analysis, and Detector Performance

Calibration of the antenna and station electronics is necessary in order to translate the recorded voltages into a measurement of the time-varying electric field vector. The gain and group delay of the analog components is measured for all channels on each RDS. The digitizers employ a self-calibration routine using a generated DC voltage, and that reference voltage is separately calibrated for each station. Frequency-dependent corrections to the digitizer DC gain have also been measured.

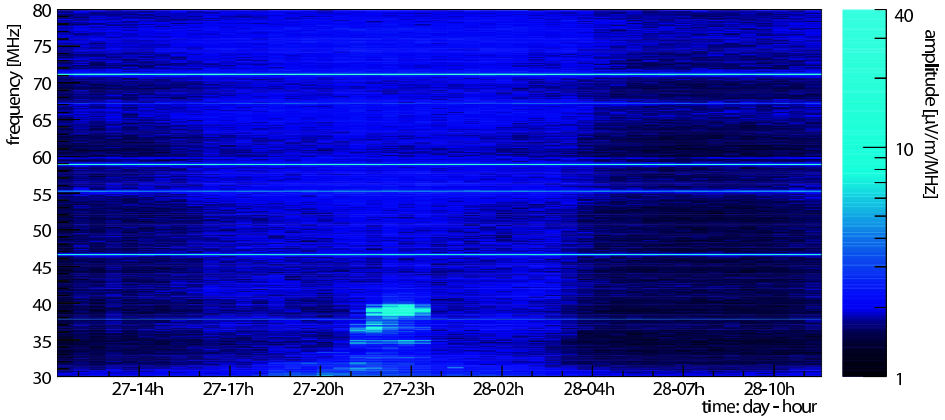

Figure 2: A daily dynamic spectrum from October 2010 — electric field strength versus frequency and time (AERA station #1, north-south polarization). The slow daily modulation of the noise level coincides with the rise and set of the Galactic Center. The calibration beacon can be seen as narrowband horizontal lines. The low-frequency noise outbursts correspond to human activity and are digitally filtered before triggering.

	Before correction (ns)	After correction (ns)
mean	2.3 ± 0.2	0.5 ± 0.1
worst	2.6	0.8

Table 1: RDS relative timing resolution measured with the beacon.

The direction- and frequency-dependent gain characteristics of the antenna are initially provided by detailed simulations. The simulation values are cross-checked using a calibrated reference transmitter that is flown over the AERA site using a tethered balloon. A full end-to-end cross-check of the calibration is planned using the same technique. Resistivity measurements of the ground conditions at AERA, which affect the antenna gain pattern, are in progress and will be incorporated into the analysis.

The OffLine analysis framework employs the station calibration data in order to reconstruct the time-varying electric field vector received at the RDS [14]. Both gain and group-delay-induced dispersion effects are corrected in the radio signals. In order to account for the directional dependence of the antenna gain, this process is iterative, with an initial reconstruction used to determine the estimated antenna gain for a specific event. The reconstruction can then be repeated to obtain more accurate electric field values.

An analysis of the beacon data has provided information on the relative stability of the GPS timing, as well as the precision possible after beacon phase correction. For this analysis, one RDS is used as a reference, and changes in the relative phase of the beacon frequencies in other stations are tracked and then corrected. The timing resolution achieved is better than 1 ns (see Table 1).

Reconstructed azimuth directions from approximately 14 hours of unfiltered data are shown in Fig. 3. The peaks correspond to RFI sources on the horizon and can easily be filtered out. These raw data can also be used to estimate the angular resolution of the first-guess reconstruction algorithm, a plane wave fit. Assuming the dominant sources are point sources on the horizon, the median space angle difference to the closest of these sources for each event is $4.2°$. As we will show in the following section, this is larger than AERA's angular resolution for more distant cosmic ray events.

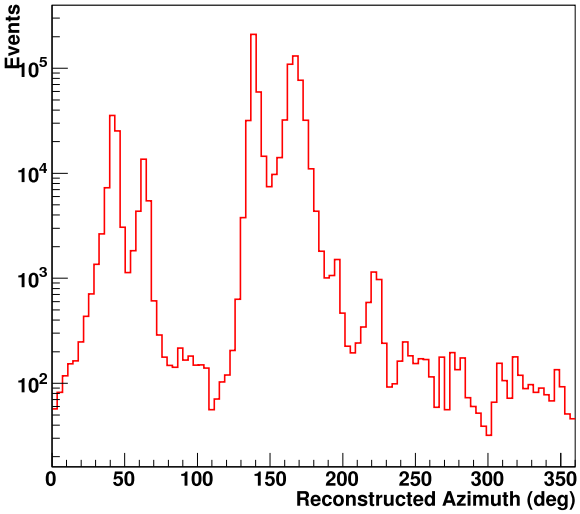

Figure 3: Reconstructed azimuth direction of 14 hours of unfiltered AERA data (8.7×10^5 events). The peaks correspond to noise sources on the horizon.

A number of reconstruction methods are under development which will further improve the angular resolution. These include:

- spherical and/or conical wave reconstructions;
- lateral distribution fits taking into account polarization effects;
- reconstructions after beacon correction; and
- localization with coherent beamforming.

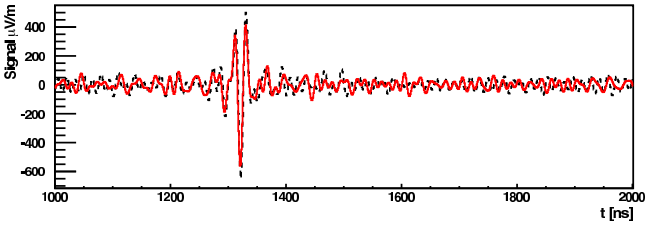

Figure 4: Calibrated radio pulse recorded for a 5.7 EeV cosmic ray event. Both north-south (solid) and east-west (dashed) polarizations are shown. The distance to the reconstructed shower axis is 114 m.

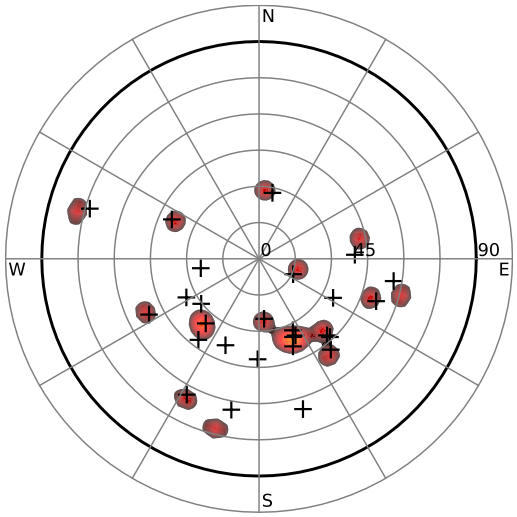

Figure 5: Polar skyplot showing reconstructed arrival directions of hybrid radio / surface detector events (the center is vertically overhead). SD directions are indicated by crosses, and for events that triggered three or more radio stations, AERA directions are shown with contours (Gaussian smearing of 3°).

4 First Hybrid and Super-Hybrid Events

The AERA Stage 1 array has been stably taking data since March 2011. Following optimization of threshold and trigger settings, the first coincident hybrid radio-SD (surface detector) events were recorded in April 2011. The rate of coincident events since then is approximately 0.3 to $0.9\,\mathrm{day}^{-1}$, depending on trigger settings and the number of stations required in coincidence. An example radio signal from a self-triggered cosmic ray event in shown in Fig. 4. A polar skyplot showing the reconstructed directions from both radio and SD is shown in Fig. 5. The median angular distance between the radio and SD reconstructions, which includes the error from the SD reconstruction, is 2.8°. The north-south asymmetry shows the dominantly geomagnetic nature of the emission, as these data were taken primarily using a trigger on the east-west polarization. This asymmetry can be reduced by also triggering on the north-south polarization. The first super-hybrid event, including fluorescence, surface detector, and radio data, was recorded on April 30, 2011, and analysis is in progress.

5 Conclusions and Outlook

Building upon the previous successes of experiments such as LOPES, CODALEMA, and prototype setups at the Auger site, AERA has demonstrated the technical feasibility of a self-triggered radio air shower array. Analysis of the first hybrid events is ongoing and will provide the necessary measurements to refine our understanding of air shower emission in the VHF band. Super-hybrid events, including data from the fluorescence detectors, will provide an accurate energy cross-calibration for both AERA and the SD infill array. Advanced reconstruction methods using the polarization and frequency characteristics of the radio pulses will soon allow tests of the energy resolution and mass determination capabilities of the radio method.

Development of hardware for Stages 2 and 3 of AERA is well underway. Selected improvements to the Stage 1 design include: a high-speed wireless communications system; large storage buffers in the RDS for sub-threshold event readout; and lower power consumption, which significantly lowers the cost per station. Within the next few years, the complete 20-km^2 array will provide the most detailed insights yet into both radio air shower physics and the cosmic ray composition at the ankle.

References

[1] K. D. de Vries et al., Astropart. Phys., 2010, **34**:267-273.
[2] T. Huege, R. Ulrich, and R. Engel, Astropart. Phys., 2008, **30**:96-104.
[3] W. D. Apel et al.(LOPES Collaboration), Astropart. Phys., 2010, **32**:294-303.
[4] D. Ardouin et al.(CODALEMA Collaboration), Astropart. Phys., 2009, **31**:192-200.
[5] T. Huege et al., Nucl. Instr. Meth. A, in press; arXiv:1009.0346.
[6] M. Platino, for the Pierre Auger Collaboration, Proc. 31st ICRC, Łódź, Poland, 2009; arXiv:0906.2354.
[7] M. Kleifges, for the Pierre Auger Collaboration, Proc. 31st ICRC, Łódź, Poland, 2009; arXiv:0906.2354.
[8] J. Coppens, for the Pierre Auger Collaboration, Nucl. Instr. Meth. A, 2009, **604**:S41-S43.
[9] C. Ruehle, for the Pierre Auger Collaboration, Nucl. Instr. Meth. A, in press (2010).
[10] B. Revenu, for the Pierre Auger Collaboration, Nucl. Instr. Meth. A, in press (2010).
[11] B. Revenu, for the Pierre Auger Collaboration, paper 0845, these proceedings.
[12] S. Buitink et al.(LOPES Collaboration), A&A, 2007, **467**: 385-394.
[13] F. G. Schröder et al., Nucl. Instr. Meth. A, 2010, **615**:277-284.
[14] P. Abreu et al.(Pierre Auger Collaboration), Nucl. Instr. Meth. A, 2011, **635**:92-102.